

This article was downloaded by: [Chonbuk National University]

On: 26 February 2013, At: 21:23

Publisher: Taylor & Francis

Informa Ltd Registered in England and Wales Registered Number: 1072954 Registered office: Mortimer House, 37-41 Mortimer Street, London W1T 3JH, UK



Liquid Crystals

Publication details, including instructions for authors and subscription information:

<http://www.tandfonline.com/loi/tlct20>

Electro-optic characteristics of the fringe in-plane switching liquid crystal device for a liquid crystal with negative dielectric anisotropy

Mi Hyeon Jo ^a, Hong Jun Yun ^a, In Won Jang ^a, Il Hwa Jeong ^a, Seung Hee Lee ^a, Sung Ho Cho ^b, Seon Hong Ahn ^b & Hae Jin Heo ^b

^a Department of BIN Fusion technology and Department of Polymer-Nano Science and Technology, Chonbuk National University, Jeonju, Korea

^b Samsung Display Co., Cheonan, Korea

Version of record first published: 12 Dec 2012.

To cite this article: Mi Hyeon Jo , Hong Jun Yun , In Won Jang , Il Hwa Jeong , Seung Hee Lee , Sung Ho Cho , Seon Hong Ahn & Hae Jin Heo (2013): Electro-optic characteristics of the fringe in-plane switching liquid crystal device for a liquid crystal with negative dielectric anisotropy, *Liquid Crystals*, 40:3, 368-373

To link to this article: <http://dx.doi.org/10.1080/02678292.2012.749307>

PLEASE SCROLL DOWN FOR ARTICLE

Full terms and conditions of use: <http://www.tandfonline.com/page/terms-and-conditions>

This article may be used for research, teaching, and private study purposes. Any substantial or systematic reproduction, redistribution, reselling, loan, sub-licensing, systematic supply, or distribution in any form to anyone is expressly forbidden.

The publisher does not give any warranty express or implied or make any representation that the contents will be complete or accurate or up to date. The accuracy of any instructions, formulae, and drug doses should be independently verified with primary sources. The publisher shall not be liable for any loss, actions, claims, proceedings, demand, or costs or damages whatsoever or howsoever caused arising directly or indirectly in connection with or arising out of the use of this material.

Electro-optic characteristics of the fringe in-plane switching liquid crystal device for a liquid crystal with negative dielectric anisotropy

Mi Hyeon Jo^a, Hong Jun Yun^a, In Won Jang^a, Il Hwa Jeong^a, Seung Hee Lee^{a*}, Sung Ho Cho^b,
Seon Hong Ahn^b and Hae Jin Heo^b

^aDepartment of BIN Fusion technology and Department of Polymer-Nano Science and Technology, Chonbuk National University, Jeonju, Korea; ^bSamsung Display Co., Cheonan, Korea

(Received 2 November 2012; final version received 11 November 2012)

Fringe-field switching (FFS) liquid crystal (LC) mode is mainly used for high-end LC displays. At present, an LC with positive dielectric anisotropy is utilised, although light efficiency of the device in a white state is not maximised due to generation of tilt angle near the edge of electrodes along the field direction. In order to overcome the demerit, an LC with negative dielectric anisotropy has been challenged. In this article, FFS mode, which shows a high light efficiency and a low operating voltage, is investigated with the utilisation of fringe in-plane electric field. The optimised device shows improved electro-optic characteristics in comparison with not only conventional LC modes, but also previously proposed FFS device using a positive type of LC.

PACS number: 42.30.R, 42.40.Ht, 42.30.Kq

Keywords: fringe-field switching, in-plane switching; transmittance; operating voltage

1. Introduction

In last 20 years, liquid crystal displays (LCDs) have been so much successful in display market, being widely used for all kinds of displays from small to large-sized displays. One of successful reasons is its improvement in image quality such that high image quality is kept in all viewing directions owing to development of many new liquid crystal (LC) modes such as wide view-twisted nematic (WV-TN) [1,2], multi-domain type of vertical alignment (MVA) [3–6], in-plane switching (IPS) [7–10] and fringe-field switching (FFS) [11–14]. At present, IPS and MVA modes are mainly used in LC-television larger than 40 inches, WV-TN in monitor, and FFS in tablet personal computers and mobiles, respectively.

Recently, LCDs are challenging to evolve further in performance and cost. In viewpoints of performances, LCDs are making efforts to increase resolution for higher image quality, improve light efficiency and reduce an operating voltage for lower power consumption. On the other hands, FFS mode is becoming a main trend being applied to all high resolution and high performance mobile, tablet, notebook, monitor and partly LCD televisions [15]. Many electro-optic studies on the FFS mode using an LC with positive dielectric anisotropy (+LC) have been reported [16–27] and at present, a LC with +LC is commercialised in the FFS-LCDs. However, the transmittance of the display is not satisfied enough as the resolution

becomes higher than 300 pixel per inch (ppi), and thus an LC with negative dielectric anisotropy (–LC) is challenged because the FFS mode with –LC shows higher transmittance than that with +LC [10,28]. In general, the magnitude of dielectric anisotropy for a commercialised is much smaller compared to that with +LC so that an operating voltage becomes higher when –LC is used.

In this article, we investigate the FFS mode with –LC which can exhibit low-operating voltage while keeping a high transmittance. The electrode structure that generates in-plane switching and fringe-field switching in voltage-on state while the LC director rotates mainly in-plane (we call the device fringe in-plane switching (FIS)) [29] is optimised to maximise electro-optic performances.

2. Cell structure and switching principle of the FIS device

Figure 1 shows comparison of electrode structures and polarity of each electrode in IPS, FFS, and FIS devices with schematic drawing of electric field lines. In the IPS device, the pixel and the common electrodes exist on the same substrate with its distance between electrodes (l) greater than its width (w) and cell gap (see Figure 1(a)), so that the in-plane electric field (E_y) is generated between the electrodes whereas no field component of E_y exists above the centre of electrodes.

*Corresponding author. Email: lsh1@chonbuk.ac.kr

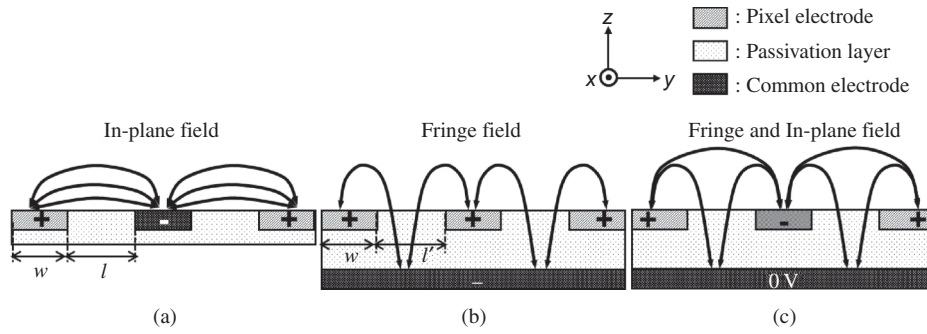


Figure 1. Cross-sectional view of electrode structures of (a) IPS, (b) FFS and (c) FIS devices with electric field lines.

In the FFS device, the slit-shaped pixel electrode with a distance (l') between electrodes and the plane-shaped common electrodes exist on the same substrate but at different layers with passivation layer between them (see Figure 1(b)). In general, the thickness of passivation layer is much lesser than the l in the IPS device, so that strong E_y near electrode surface is induced in between pixel and common electrodes when the same voltage as that in the IPS device is applied whereas fringe electric field having both E_y and E_z between edge and centre of the pixel electrode exists and no field component of E_y exists above centre of the pixel and the common electrodes. In the FIS device, the cross-sectional view of the electrode structure is the same as in the FFS device except that the nearby pixel electrodes are supposed to have different levels of voltages, whereas the common electrode kept a certain DC level. In other words, the alternative pixels in the FIS device are driven by a couple of distinct oscillating signals, one in out of phase with the other and the common electrode is biased at certain fixed DC level [29]. In this way, fringe electric field exists between pixel and common electrodes and, at the same time, E_y exists even in between pixel electrodes. In the FFS device, there are two electrode positions, centre of pixel electrode and centre of between pixel electrodes without a field component E_y , however, there is only one electrode position, centre of pixel electrode in the FIS device.

Now, let us consider light modulation associated with the proposed device. When a LC is homogeneously aligned between two crossed polarisers and light modulation of the device is mainly dependent on phase retardation method, the normalised optical transmittance of the device is given as

$$T/T_0 = \sin^2 2\Phi(V) \sin^2 \pi d \Delta n_{\text{eff}}(V)/\lambda \quad (1)$$

where $\Phi(V)$ is voltage-dependent angle between the LC optic axis and the transmission axis of the polariser, d is a cell gap and Δn_{eff} is effective birefringence of the LC at a given voltage V and wavelength

λ . In both FFS and FIS devices, the LC directors are homogeneously aligned with $\Phi = 0^\circ$ at $V = 0$ and thus the cell appears dark. As the voltage exceeds a threshold, the field rotates LC directors to generate Φ and Δn_{eff} so that the incident light transmits through the crossed analyser. According to Equation (1), in order to maximise the transmittance, Φ should be 45° , that is, LC director should rotate by 45° . Since the field component to rotate LC director is mainly E_y so that the LC director may not rotate enough at electrode positions where E_y does not exist such as above centre of electrodes in IPS device, above centre of pixel electrodes and centre of between pixel electrodes in FFS device and above centre of pixel electrodes in FIS device, resulting in relatively low transmittance compared to other electrode positions.

3. Results and discussion

Optimisation of the cell and electrode structure in the FIS device has been performed based on simulation. For calculation purposes, we used the commercially available 'LCD master' (Shintech, Japan) software, where the motion of LC directors is calculated by the Eriksen–Leslie theory and 2×2 extended Jones Matrix method [30] is applied for optical transmittance calculation.

In order to compare electro-optic performances between FFS and FIS modes, conventional electrode structure with (w) = $3.0 \mu\text{m}$ and $l' = 4.5 \mu\text{m}$ is chosen. The LC physical properties such as birefringence (Δn) is 0.08 at 589.3 nm, dielectric anisotropy ($\Delta\epsilon$) = -4.0 , elastic constants, namely splay $K_{11} = 13.5 \text{ pN}$, twist $K_{22} = 6.5 \text{ pN}$, bend $K_{33} = 15.1 \text{ pN}$ and rotational viscosity (γ_1) = $104 \text{ mPa}\cdot\text{s}$, have been used for simulation. The surface pre-tilt angle for both substrates has been chosen to be 2° and the LC director maintains 10° with respect to E_y . The cell gap is $4.0 \mu\text{m}$. Figure 2 shows voltage-dependent transmittance (V-T) curves and transmittance profile along electrode position. As clearly indicated in Figure 2(a), the operating voltage is only 2.7 V, whereas in the FFS it is 4.7 V,

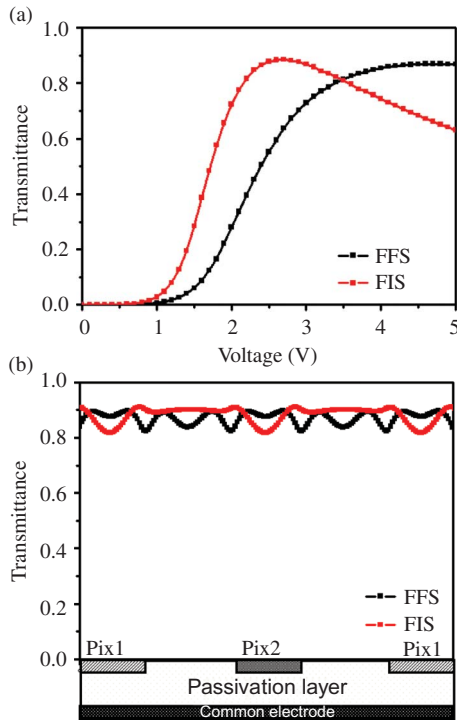


Figure 2. (a) Comparison of voltage-dependent transmittance curves and (b) transmittance profile along electrode positions in FFS and FIS devices. Here “Pix” indicates a pixel electrode.

indicating a strong advantage of the FIS mode over the FFS mode in the driving voltage. And the normalised transmittance also increases from 0.869 to 0.884, respectively, so high enough to show about 95% of TN mode. To confirm the transmittance difference between two modes, the transmittance has been calculated along the y direction, as shown in Figure 2(b). The oscillation level of transmittance is slightly reduced in the FIS mode compared to that in the FFS mode because E_y exists even in the centre between pixel electrodes; however, the transmittance is slightly lowered above pixel electrodes in the FIS mode because there is no E_y , as explained in the switching principle part.

In order to optimise retardation value of the LC layer, the electro-optic characteristics of the proposed device has been simulated with fixed thickness but varying birefringence value of LC, which leads to the variation of LC’s retardation from 320 to 350 nm in steps of 10 nm at previously mentioned cell conditions. The simulation results exhibit maximum transmittance for the device at retardation value of 340 nm; however, the operating voltage remains invariant with the variation of cell retardation as depicted in Figure 3.

Now, optimisation of the distance l' between pixel electrodes is performed. In the FFS mode, an optimal ratio of l'/w , which shows high transmittance and

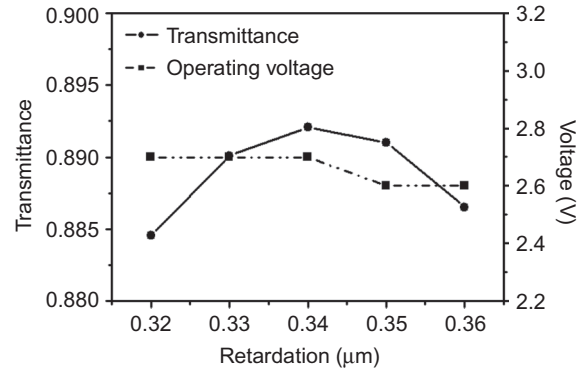


Figure 3. Operating voltage and maximum transmittance curves of the FIS device as a function of cell retardations.

proper operating voltage, is in the range of 1.5–2.5. According to our previous report, if the ratio becomes larger, the non-uniformity in transmittance difference in grey scale from position to position is reduced, although there is mispatterning of electrodes [31]. Therefore, larger l' is favoured in terms of fabrication viewpoints.

The variation of device transmittance and operating voltage as a function of intra pixel separation l' of proposed FIS device at fixed w with 3 μm has been depicted in Figure 4. Here, the phase retardation of the FIS device is chosen to be 340 nm. The l' has been varied from conventional 4.5 to 9.0 μm in steps of 1.5 μm . As a result, the operating voltage shows an increasing trend with widening the l' because the intensity of E_y between two pixel electrodes decreases with increasing l' . Interestingly, the transmittance also increases with increasing l' up to 6.0 μm , but further increment is found to reduce transmission. The electro-optic performance of the proposed device with optimal conditions for $l' = 6.0 \mu\text{m}$ and $w = 3 \mu\text{m}$ is excellent such that the transmittance reaches 0.90 and the operating voltage is only 3.1 V.

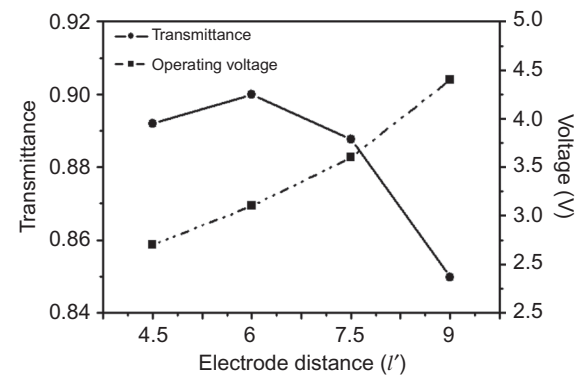


Figure 4. Operating voltage and maximum transmittance curves of the FIS device according to l' at $w = 3.0 \mu\text{m}$.

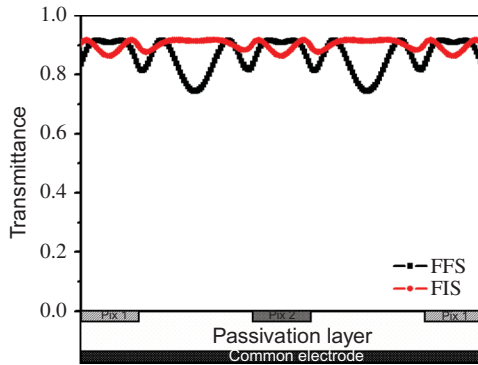


Figure 5. Comparison of electrode-position-dependent transmittance between FFS and an optimised FIS device.

We also investigated transmittance of the device along electrode positions for $l' = 6.0 \mu\text{m}$ and $w = 3 \mu\text{m}$ and compared with that in FFS mode, as shown in Figure 5. The transmittance is found to oscillate according to electrode positions; however, the difference of transmittance at FIS mode is much less than that in FFS mode. In FFS mode, transmittance decreases quite much at between two pixel electrodes in which the LC reorients by elastic torque between neighbouring LC molecules. Therefore, increasing l' in FFS mode to improve process margin is disadvantageous in achieving high transmittance. The simulation result shows evenly distributed transmittance over the whole positions such that the difference of transmittance in accordance with electrode positions is almost negligible.

The performance of FIS device using $-LC$ have been further analysed by simulating LC director configuration in accordance with electrode position at operating voltage as shown in Figure 6. Twist and tilt angles at five different positions are calculated since the transmittance oscillates with a repeated unit with an electrode distance from A to E . The maximal twisted angle from the initial position is strongly dependent on electrode position such that it is about 57° at $z/d = 0.28$ for position C and 45° at $z/d = 0.40$, 49° at $z/d = 0.38$, 54° at $z/d = 0.43$ and 50° at $z/d = 0.50$ for position A , B , D and E , respectively. It seems that the light modulation follows polarisation rotation at C and phase retardation at A , B , D and E in the FIS mode [29]. In addition, Φ is over 45° with suppressed tilt angles less than 12° at all electrode positions, indicating that the transmittance is maximised over whole position and the LC director rotates mainly in plane. As a result, the FIS device also exhibits wide viewing angle like in the FFS device.

Finally, voltage-dependent transmittance curves between IPS, FIS and FFS devices are compared, as

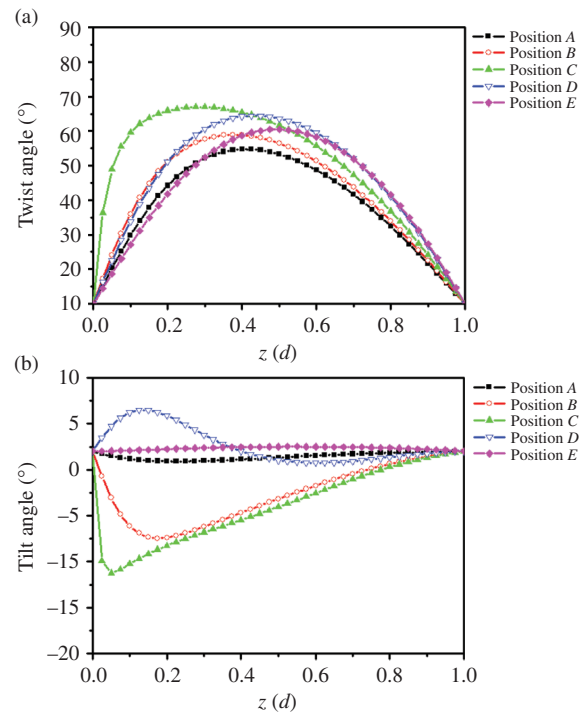


Figure 6. LC director profiles of the FIS device at five different positions A , B , C , D and E : (a) twist and (b) tilt angles in a white state.

shown in Figure 7, where w is $3.0 \mu\text{m}$ and the distance between electrodes is $6.0 \mu\text{m}$ with retardation values 0.32 , 0.34 and $0.36 \mu\text{m}$, respectively. The cell gap and physical properties of LC is the same as those mentioned above. In the FIS device, transmittance is higher and operating voltage is lower than FFS and IPS devices. The maximum transmittances of FIS, FFS and IPS devices are 0.90 , 0.88 and 0.83 , and driving voltages are 3.1 , 4.5 and 5.7 V, respectively, indicating high transmittance as well as low operating voltage, can be achieved in the FIS device.

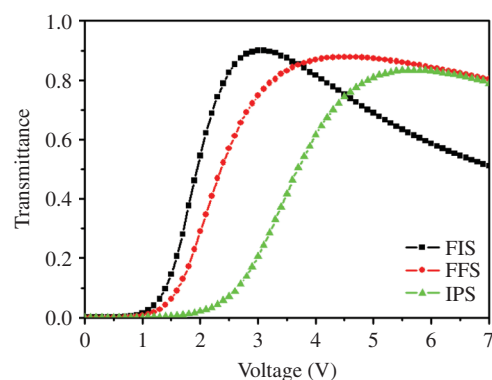


Figure 7. Comparison of voltage-dependent transmittance curves in FIS, FFS and IPS devices.

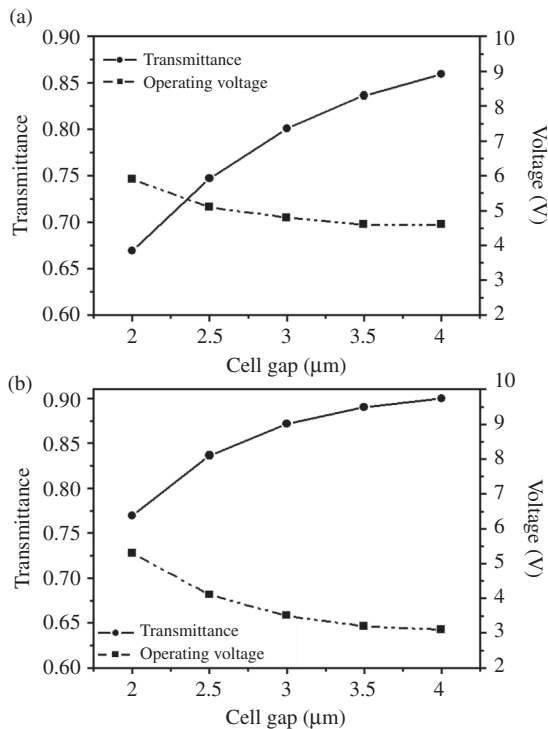


Figure 8. Transmittance and operation voltage as a function of cell gap in (a) FFS and (b) FIS devices.

On the other hand, the transmittance and operating voltage of the FFS device generally decrease and increase as the cell gap decreases. Figure 8 shows maximum transmittance and operating voltage as a function of cell gap in the FFS and FIS mode. In the FFS mode, as the cell gap decreases from 4 to 3 μm and to 2 μm , the operating voltage increases from 4.6 to 4.8 V and to 5.9 V, and the transmittance decreases from 0.86 to 0.80 and to 0.67, respectively. However, in the FIS device, the operating voltage also increases from 3.1 to 5.3 V and the normalised transmittance decreases from 0.90 to 0.77 with decreasing the cell gap from 4 to 2 μm , but the dropping ratio of transmittance is much lower in the FIS than in the FFS device. Consequently, the FIS device has advantages in electro-optic performances over the FFS mode even in low cell gap cell for achieving fast response times.

One disadvantage of the FIS device is that it might need two transistors to apply different level of signals to each pixel electrode, which results in reduction of an aperture ratio. The advantages of the device in improved transmittance and reduced operating voltage need to be compared with disadvantage in real fabrication.

4. Summary

We have studied electro-optic performances of the device, which utilises fringe and in-plane field using

a -LC and compared with conventional IPS and FFS devices. Electrode structure and cell retardation that exhibit maximal transmittance and optimal operating voltage have been achieved. The optimised device can show higher transmittance and lower operating voltage than those of the FFS mode, which might open low power consumption LC device while keeping wide viewing angle.

Acknowledgments

M.H. Jo, H.J. Yun, I.W. Jang, I.H. Jeong and S.H. Lee thank the World Class University programme (R31-20029) funded by the Ministry of Education, Science and Technology and also the Samsung Display Corporation for financial support.

References

- [1] Mori H. Novel optical compensators of negative birefringence for wide-viewing-angle twisted-nematic liquid-crystal displays. *Jpn J Appl Phys.* 1997;36:1068–1072.
- [2] Mun B-J, Lim D-E, Kang, Lim YJ, Lee SH, Lee G-D. A wide-view twisted nematic liquid crystal cell with improved image quality obtained by decreasing γ -curve distortion. *J Mod Optics.* 2012;59(14):1204–1208.
- [3] Takeda A, Kataoka S, Sasaki T, Chida H, Tsnda H, Ohmuro K, Koike Y, Sasabayashi T, Okamoto K. A super-high image quality multi-domain vertical alignment LCD by new rubbing-less technology. *SID int Symp Dig Tech Pap.* 1998;29:1077–1080.
- [4] Hanaoka K, Nakanishi Y, Inoue Y, Tanuma S, Koike Y. A new MVA-LCD by polymer sustained alignment technology. *SID Int Symp Dig Tech Pap.* 2004;35:1200–1203.
- [5] Kim SG, Kim SM, Kim YS, Lee HK, Lee SH, Lee G-D, Lyu J-J, Kim KH. Stabilization of the liquid crystal director in the patterned vertical alignment mode through formation of pretilt angle by reactive mesogen. *Appl Phys Lett.* 2007;90:261910–1–3.
- [6] Lee SH, Hong SH, Kim JM, Kim HY, Lee JY. An overview of product issues in wide-viewing TFT-LCDs. *J Soc Inf Disp.* 2001;9:155–160.
- [7] Oh-e M, Kondo K. Electro-optical characteristics and switching behavior of the in-plane switching mode. *Appl Phys Lett.* 1995;67:3895–3897.
- [8] Oh-e M, Kondo K. Quantitative analysis of cell gap margin for uniform optical properties using in-plane switching of liquid crystals. *Jpn J Appl Phys.* 1997;36:6798–6803.
- [9] Jung BS, Baik IS, Song IS, Lee G-D, Lee SH. Study on colour characteristics depending on orientation of liquid crystal in the in-plane switching mode. *Liq Cryst.* 2006;33:1077–1082.
- [10] Ge Z, Zhu TX, Wu S-T. High transmittance in-plane switching liquid crystal displays. *J Disp Tech.* 2006;2:114–120.
- [11] Lee SH, Lee SL, Kim HY. Electro-optic characteristics and switching principle of a nematic liquid crystal cell controlled by fringe-field switching. *Appl Phys Lett.* 1998;73:2881–2883.

- [12] Lee SH, Lee SL, Kim HY, Eom TY. Novel wide-viewing-angle technology: ultra-trans view. *SID Int Symp Dig Tech Pap.* 1999;30:202–205.
- [13] Lee SH, Lee SM, Kim HY, Kim JM, Hong SH, Jeong YH, Park CH, Choi YJ, Lee JY, Koh JW, Park HS. 29.2:18.1" Ultra-FFS TFT-LCD with super image quality and fast response time. *SID Int Symp Dig Tech Pap.* 2001;32:484–487.
- [14] Lee SH, Kim HY, Lee SM, Hong SH, Kim JM, Koh JW, Lee JY, Park HS. Ultra-FFS TFT-LCD with super image quality, fast response time and strong pressure-resistant characteristics. *J Soc Inf Disp.* 2002;10:117–122.
- [15] Lee SH, Bhattacharyya SS, Jin HS, Jeong K-U. Devices and materials for high performance mobile liquid crystal displays. *J Mater Chem.* 2012;22(24):11893–11903.
- [16] Lee SH, Lee SL, Kim HY, Eom TY. Analysis of light efficiency in homogeneously aligned nematic liquid crystal display with interdigital electrodes. *J Kor Phys Soc.* 1999;35:S1111–S1114.
- [17] Hong SH, Park IC, Kim HY, Lee SH. Electro-optic characteristic of Fringe-Field switching mode depending on rubbing direction. *Jpn J Appl Phys.* 2000;39:L527–L530.
- [18] Kim HY, Nam S-H, Lee SH. Dynamic Stability of the Fringe-Field Switching Liquid Crystal Cell Depending on Dielectric Anisotropy of a Liquid Crystal. *Jpn J Appl Phys.* 2003;42:2752–2755.
- [19] Kim HY, Hong SH, Rhee JM, Lee SH. Analysis of cell gap-dependent driving voltage in a fringe field-driven homogeneously aligned nematic liquid crystal display. *Liq Cryst.* 2003;30(11):1285–1292.
- [20] Jung SH, Kim HY, Kim JH, Nam SH, Lee SH. Analysis of optimal phase retardation of a fringe field-driven homogeneously aligned nematic liquid crystal cell. *Jpn J Appl Phys.* 2004;43(3):1028–1031.
- [21] Kim SJ, Kim HY, Lee SH, Lee YK, Park KC, Jang J. Cell gap-dependent transmittance characteristic in a fringe field-driven homogeneously aligned liquid crystal cell with positive dielectric anisotropy. *Jpn J Appl Phys.* 2005;44:6581–6586.
- [22] Kim MS, Seen SM, Jeong YH, Kim HY, Kim SY, Lim YJ, Lee SH. Effect of horizontal electric field generated by data signal on disclination lines near pixel edge in fringe field switching mode. *Jpn J Appl Phys.* 2005;44:6698–6700.
- [23] Lim YJ, Lee MH, Lee GD, Jang WG, Lee SH. A single-gap transfective fringe field switching display using a liquid crystal with positive dielectric anisotropy. *J Phys D Appl Phys.* 2007;40:2759–2764.
- [24] Kim MS, Seen SM, Lee SH. Control of reverse twist domain near a pixel edge using strong vertical electric field in the fringe-field switching liquid crystal device. *Appl Phys Lett.* 2007;90:133513–1–3.
- [25] Ge Z, Wu S-T, Kim SS, Park JW, Lee SH. Thin cell gap fringe field switching liquid crystal display with chiral dopant. *Appl Phys Lett.* 2008;92:181109–1–3.
- [26] Ryu JW, Lee JY, Kim HY, Park JW, Lee GD, Lee SH. Effect of magnitude of dielectric anisotropy of a liquid crystal on light efficiency in the fringe-field switching nematic liquid crystal cell. *Liq Cryst.* 2008;35:407–411.
- [27] Jung JH, Ha KS, Srivastava AK, Lee HK, Lee SE, Lee SH. Light efficiency of the fringe-field switching mode depending on magnitude of dielectric anisotropy of liquid crystal associated with cell gap and rubbing angle. *J Kor Phys Sci.* 2010;56:548–553.
- [28] Yun HJ, Jo MH, Jang IW, Lee SH, Ahn SH, Hur HJ. Achieving high light efficiency and fast response time in fringe field switching mode using a liquid crystal with negative dielectric anisotropy. *Liq Cryst.* 2012;39:1141–1148.
- [29] Park JW, Ahn YJ, Jung JH, Lee SH, Lu R, Kim HY, Wu ST. Liquid crystal display using combined fringe and in-plane electric fields. *Appl Phys Lett.* 2008;93:081103–1–3.
- [30] Lien A. Extended Jones matrix representation for the twisted nematic liquid-crystal display at oblique incidence. *Appl Phys Lett.* 1990;57:2767–2769.
- [31] Eom TY, Ryu SK, Kang SK, You JG, Lim YJ, Lee SH. Study of high tolerant pixel structure due to mispatterning of electrodes for the fringe-field switching liquid crystal display. *Jpn J Appl Phys.* 2009;48:101602–1–4.